DOI: 10.17277/amt.2016.01.pp.017-028

# Effect of Fullerenes $C_{60}$, $C_{70}$ and CNTs on the Thermophysical Properties of Nitrogen- and Oxygen-Containing Liquids (Rocket Fuel)

M.M. Safarov[a]*, N.B. Davlatov[b], M.M. Gulomov[b], M.A. Zaripova[b]

[a] *National Research University "Moscow Power Engineering Institute", Branch in Dushanbe, Dushanbe, Tajikistan Republic*
[b] *M.S. Osimi Tajik Technical University, 10, Academicians Rajabov St., Dushanbe, 734042, Tajikistan Republic*

* Corresponding author: Tel.: +7 992 37 221 35 11. *E-mail*: ttu@ttu.tj

**Abstract**

The paper presents the results of the experimental research of thermal properties (thermal conductivity, heat capacity, density and temperature diffusivity) of nitrogen- and oxygen-containing liquids in pure form and in the form containing 0.5 % fullerene-like carbons and carbon nanotubes with diameter $d$ = 40 nm, 50 nm, 60 nm) in the temperature range 293–453 K and in the pressure range 0.101–49.01 MPa. To measure thermal conductivity, heat capacity and temperature diffusivity, special setups designed by professors E.S. Platunov, M.M. Safarov and I.F. Golubev were used. The computer-aided method of monotonous heating and regular thermal first-order regime was applied. The total relative error of measuring thermal conductivity, heat capacity, density and temperature diffusivity was equal to 2.6, 3.4, 0.1, 4.5 % when confidence probability $\alpha = 0.95$. Using the law of corresponding states and experimental data on thermal conductivity, heat capacity, density and temperature diffusivity of the samples, the empirical equation for calculating the thermophysical properties of unexplored liquids under different temperatures and pressures was obtained.

**Keywords**

Density; heat capacity; method of monotonous heating; nitrogen- and oxygen-containing liquids; regular thermal regime of the first kind; temperature diffusivity coefficient; thermal conductivity.



## Introduction

Nanofluids being produced have to meet certain requirements. They should be uniform, resistant to agglomeration and precipitation for a long time; they should be free of chemical reactions, etc. According to many authors, the main problem is agglomeration. It should be noted that the tendency towards agglomeration reflects one of the most important properties of nanoparticles – their high surface activity. On the one hand, high surface activity of nanoparticles allows the smaller particles do not sink (not to precipitate), and, on the other hand, they tend to form agglomerates. This feature of nanoparticles significantly affects the technologies for nanofluids producing and keeping them in operation condition.

Two crystalline allotropic modifications of carbon (graphite and diamond) have been known since ancient times. As early as 1973 D.A. Bochvar and E.N. Galperin proposed that a closed polyhedron of carbon atoms in the form of a truncated icosahedron might have a closed electron shell and high binding energy. However, this work was not accepted by scientific community, and only in 1985 H. Kroto with his co-workers discovered an intensive peak with a mass of 720 u in the mass-spectrum of graphite decomposition products under the laser beam. This fact was explained by the presence of $C_{60}$ molecules. The other less intensive peak with a weight of 840 u was associated with $C_{70}$ molecule. The fascinating story of this discovery was detailed in Kroto, Smalley and Curl's Nobel lectures. A new allotropic modification of carbon was called "fullerene". In 1990 Krätschmer's method for producing fullerenes in macroscopic quantities led to the intensive studies and emergence of new trends in solid-state physics, chemistry of aromatic compounds and molecular electronics.

Fullerenes are resistant polyhydric carbon clusters with the amount of atoms from several dozens or

more. The number of carbon atoms in such a cluster is not random, and complies with certain laws. The form of fullerenes is a spheroid, the faces of which form pentagons and hexagons. According to the Euler's geometrical calculations, to construct such a polyhedron the number of pentagonal faces should be twelve, the number of the hexagonal faces can be chosen arbitrarily. Such a requirement is met by clusters with the number of atoms $n$ = 32, 44, 50, 58, 60, 70, 72, 78, 80, 82, 84 etc. Owing to its highest stability and symmetry, fullerene $C_{60}$ is of great interest from the experimental point of view.

Numerous experimental and theoretical papers on various aspects of the physics of $C_{60}$ in different states (an isolated molecule, $C_{60}$ in solutions, and especially $C_{60}$ in the solid state) have already been published. $C_{60}$ forms molecular crystals at temperatures below 600 K. Crystals of high purity (99.98 %) and of millimeter sizes may be grown from the gaseous phase. Isolated $C_n$ molecules are called fullerenes; fullerites are fullerenes in the solid state, including polymerized fullerene structures. Diversified fullerene derivatives include intercalated compounds and endohedral fullerenes. Intercalation allows introducing impurities into the cavities of the fullerite crystal lattice and endohedral fullerenes are formed while different kinds of atoms are introduced into a $C_n$ cluster.

From the chemical point of view, fullerenes can be considered as three-dimensional analogues of planar aromatic compounds, but with the important difference: the conjugation with an electronic system is permanent. Fullerenes do not contain hydrogen which can participate in a substitution reaction. There are two types of chemical reactions with fullerenes: addition reactions and redox reactions, leading to covalent exohedral compounds and salts, respectively. If one could find a chemical reaction, which would open a window in a fullerene cage, allowing injection of a small molecule or atom and further regeneration of the cluster, one can get a method of endohedral fullerenes obtaining. However, the majority of endohedral metal fullerenes are being generated either in the presence of a alien substance, or by implantation.

The most efficient method of fullerenes production is based on thermal decomposition of the graphite. If graphite is heated moderately, the bond between the individual layers of graphite is broken, but vaporized material does not decompose into single atoms. Such vaporized layer consists of individual fragments that are a combination of hexagons. These fragments build $C_{60}$ molecule and other fullerenes. For decomposition of graphite in the preparation of fullerenes we can use resistive and high-frequency heating of a graphite electrode, combustion of hydrocarbons, laser irradiation of a graphite surface, evaporation of graphite by a focused sunbeam. These processes are carried out in a buffer gas and helium is commonly used as such. Arc discharge with graphite electrodes in a helium atmosphere is mostly used to obtain fullerene. The main role of helium is associated with the cooling of fragments that have high degree of vibrational excitation, which prevents their integration into a stable structure. Optimum pressure of helium is in the range of 50–100 Torr. The basis of the method is simple: an electric arc with an evaporating anode is ignited between two graphite electrodes. The carbon black, containing from 1 to 40 % (depending on the geometric and technological parameters) of fullerenes, sets out on the walls of the reactor. For extracting fullerenes from the fullerene-containing carbon black, their separation and purification, the solvent extraction and column chromatography are used. At the first stage the carbon black is treated by non-polar solvent (toluene, xylene, carbon disulfide). The extraction efficiency is achieved by using Soxhlet extractor or by ultrasonication. The obtained solution of fullerenes is separated from the residue by filtration and centrifugation, the solvent is distilled or evaporated. The solid residue comprises a mixture of fullerenes, in varying degrees of solvated solvent. Separation of fullerenes into the individual compounds is carried out by means of column liquid chromatography or high pressure liquid chromatography. Complete removal of the solvent from the solid sample of fullerene is carried out by keeping it at 150–250 °C under dynamic vacuum for several hours. Further increase in purity degree is achieved by sublimation of purified samples.

Experimental studies of effective thermal conductivity of such nanofluids as: gold + toluene, aluminum oxide + water, titanium oxide + water, copper oxide + water, carbon nanotube + water are presented in [26]. The diameters of these spherical particles were respectively 1, 65, 20, 40 and 33 nm; the average length and diameter of carbon nanotubes were $10^{-6}$ m and 150 nm. The author's measurement results [26] have shown that the effective thermal conductivity of nanofluids is not abnormally high, and with good accuracy can be predicted by the model [6] for spherical nanoparticles and with the help of Yamada and Ota's single-cell model for carbon nanotubes [26].The most detailed analysis of the revealed unusual properties of nanofluids is given in the review [27]. In addition to strong growth of thermal conductivity with a low concentration of nanoparticles, the author indicates other important properties of nanofluids that distinguish them from conventional suspensions. In particular, they include the

nonlinear dependence of thermal conductivity on the concentration of the nanoparticles and its strong dependence on temperature and particle size. Non-linear dependence between thermal conductivity and concentration of particles was first found while researching carbon nanotubes-oil nanofluids [28]. Strong dependence of thermal conductivity of nanofluids on temperature and particle size was described in a number of papers. Measurement results obtained by different authors were classified according to the nanoparticles material. Water, ethylene glycol, oil, and polymers-based composite materials were used as the base liquids. Also, the materials of nanoparticles were different. They included multi-walled carbon nanotubes, gold, copper, silicon carbide, aluminium oxide and titanium. It is well known that particles tend to agglomerate and this process affects thermal conductivity of the fluid. It was shown that the presence of nanoparticles in liquids greatly increases thermal conductivity, besides the scale of increasing thermal conductivity depends on the material of nanoparticles and their volume fraction. Thus, while some experimental results testify to the anomalous behavior of thermal conductivity, others confirm common understanding of suspensions. Such a controversy between different authors' data is due to a wide variety of factors affecting thermal conductivity of nanofluids and necessitates further accumulation of experimental data and their systematization.

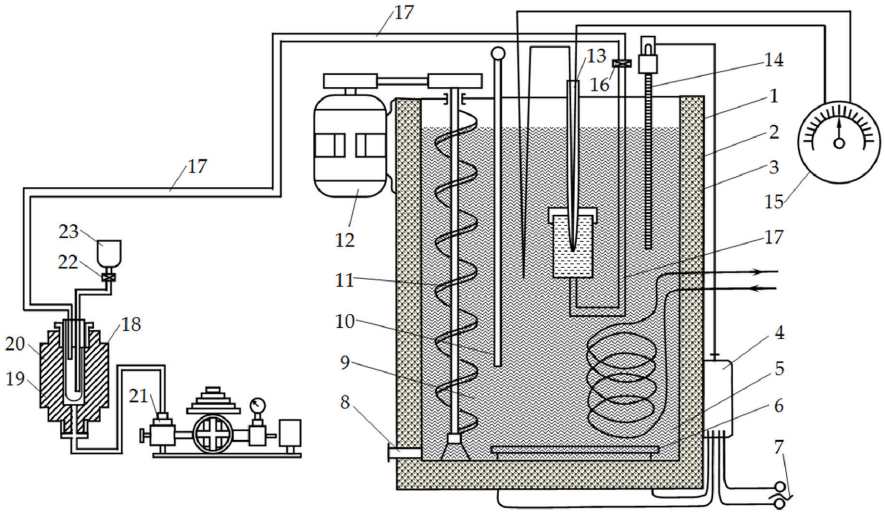


**Fig. 1. The setup for determining the thermophysical properties (λ, $C_p$, *a*) for high state parameters**:
*1* – cylindrical vessel; *2* – insulator; *3* – outer vessel; *4* – electric network; *5* – coil for cooling; *6* – heater; *7* – thermostat; *9* – thermostating liquid; *10* – thermometer; 11 – auger-mixer; *12* – electric motor; *13* – a-calorimeter; *14* – contact thermometer; *15* – galvanometer; *8*, *16*, *22* – valves; *17* – stainless metal tube; *18*, *19* – pressure vessels; *20* – polyethylene bags; *21* – deadweight pressure tester MP-2500; *23* – metallic glass to fill the testing liquid or solution

## 2. The experimental

### 2.1. *The experimental setup for measuring thermophysical properties (λ, $C_p$, a) of solutions and liquids under different temperatures and pressures*

To measure the coefficient of temperature diffusivity, thermal conductivity and heat capacity of liquids under different temperatures and pressures, an experimental setup was used according to the method of regular thermal regime [2, 12–15] (Fig. 1) and density (Fig. 2 and 3).

This setup (Fig. 1) consists of a cylindrical vessel *1*, placed inside the outer vessel *3* filled with thermostatic liquid *9*, which is placed in a medium calorimeter *13*. The receptacles are divided by an insulator *2*. The device comprises a coil for cooling *5*; a heater *6* for heating and setting experimental temperature; a thermostat *7* to protect from overheating; a valve *8* for a drain of thermostating liquid; a thermometer *10* for monitoring the temperature; an auger-mixer *11* for the active fluid mixing and equalization of the temperature gradient; an electric motor *1* for rotating the screw; a contact thermometer *14* to set the temperature of the experiment; a galvanometer *15*; an electric network *4*. To create the pressure of liquid the device is provided with a pressing vessel *18* and a deadweight pressure tester MP-2500 *21*. A pressing vessel *18* and a calorimeter *13* are connected by stainless steel tubes *17*. To perform the experiment a stopwatch is required.

To monitor the temperature of a-calorimeter we used a differential chrome-aluminum thermocouple with a diameter of 0.15 mm, the ends of which were connected to a galvanometer *15*. A cold junction of the differential thermocouple was placed into the thermostating liquid and a hot junction – into the center of a-calorimeter *13*. The calculations showed that confidence limit error of thermal conductivity measured by regular thermal regime of the first kind in a relative form at $\alpha = 0.95$ was equal to 1.9 %, procedure error was 0.4 %, instrumental error was 1.1 %. The total relative measurement error was 3.4 %.

### 2.2. *Method for measuring thermophysical properties (λ, $C_p$, a) of solutions and liquids under different temperatures and pressures*

In the closed position of valves *16*, *22* the test liquid is poured into a glass *23*, then valves *22*, *16* are opened and when the calorimeter is filled with the liquid, they are closed. Before the experiment the liquid in the setup is degassed by means of heating the experimental device up to the boiling point at the open position of the high pressure valve *23*. The stationary thermal condition under the given temperature of the experiment is set after the heating. The required pressure is created by the MP-2500 deadweight pressure tester through the pressure vessel of the device. Then the calorimeter with the test material and fixed thermocouple is heated to a certain temperature and put into a thermostat. During the setting of the regular mode the change in the temperature is observed. If the object is cooled under a constant temperature, provided the heat transfer coefficient is relatively high, then for the period of the regular regime the cooling graph of the object (in semi-logarithmic coordinates it is designated as $\ln(\Delta T) = f(\Delta\tau)$) is represented in the form of a straight line. According to this graph, you can find the index (rate) of cooling ($m$) through the ratio [2, 11–15, 17]:

$$m = \ln(\Delta T)/\Delta\tau, \quad (1)$$

where $\Delta T$ is a difference between the temperature at some point of the test object and the constant ambient temperature (thermostating liquid); $\Delta\tau$ is the cooling time.

K.M. Kolarov's [2] experimental setup, shown in Fig. 1, is used to determine the temperature diffusivity of dairy products and tomato pastes [2].

After being upgraded by us, the Kolarov's setup allows measuring the temperature diffusivity of the analyzed nanofluids, solutions, liquids under different temperature and pressure conditions.

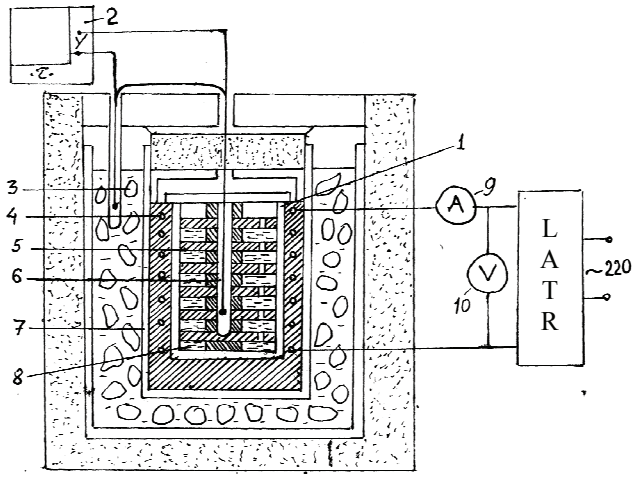


**Fig. 2. The experimental setup for measuring the specific heat of liquids and solutions depending on the temperature under the atmospheric pressure**

The coefficient of temperature diffusivity by the method of two points is determined by the formula [2, 6]:

$$a = Fm, \quad (2)$$

where $m$ – is cooling rate, 1/s – is determined by the formula used for the thermal conductivity determination; $F$ – is the value that takes into account the shape and size of a-calorimeter [2].

$$F = \frac{1}{\left(\frac{2,405}{R}\right)^2 + \left(\frac{\pi}{l}\right)^2} = 0,34 \cdot 10^{-4} \ \text{m}^2, \quad (3)$$

where $R$ and $l$ are the radius of the cylinder and its height, respectively.

To calculate the thermal conductivity coefficient of colloidal solutions the following formula was used:

$$\lambda = AC_p m, \quad \text{W/(m·K)}, \quad (4)$$

where $A$ – the coefficient of the calorimeter form, obtained during the setup calibration; $C_p$ – specific heat capacity of the reference sample; $m$ – the cooling rate (1/s) was determined by formula (1).

By thermal diffusivity, thermal conductivity and density of the solutions under various temperatures and pressures the specific heat of test solutions was calculated using the formula:

$$C_p = \frac{\lambda}{\rho a}, \ \frac{\text{J}}{(\text{kg} \cdot \text{K})}. \quad (5)$$

### 2.3. *The experimental setup for measuring specific heat capacity of solutions depending on the temperature under atmospheric pressure*

The experimental setup for measuring specific heat of liquids under the temperature range of 273–473 K and atmospheric pressure was developed by M.M. Safarov. According to the method of monotonous heating, the setup (Fig. 2) consists of a calorimeter *1*, a graph plotter *2*, a container with melting ice *3* and electrical measuring instruments *9*, *10* [14].

The calorimeter consists of a metal cylinder on the outer surface of which the heater is wound *4*. Inside the cylinder the intermediate core of calorimeter in the form of a cylindrical radiator *5* with a high thermal conductivity is located. The grooves of the core are filled with test liquid, and along the axis there is a hot junction of the differential thermocouple *6*. The calorimeter is insulated from

outside with asbestos and placed in a copper cylinder *7* and its temperature is equal to the temperature of melting ice [33].

Such a construction of the calorimeter allows measuring the heat capacity of liquids during monotonous heating. The presence of the intermediate core in the form of a radiator *5* excludes the influence of thermal conductivity of the liquid on the measurements in this condition.

The experiment is carried out in the following order. The calorimeter is filled with test liquid *8* and a copper cylinder is placed into the ice-water mixture *3*. The calorimeter is kept for one hour under the temperature of melting ice to achieve the thermodynamic equilibrium. Then the heater of calorimeter is switched on *4* and simultaneously the graph plotter H-3306 *2* starts. Its X-axis represents the time and Y-axis fixes the temperature of the calorimeter.

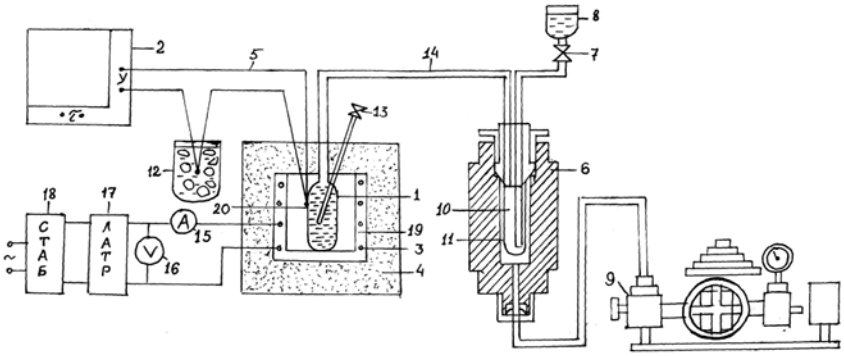


**Fig. 3.The experimental equipment for measuring the heat capacity of liquids and solutions under high state parameters:**
*1* – metal vessel; *2* – the H-306 graph plotter; *3* – nichrome heater; *4* – heat-insulating layer (asbestos); *5* – chrome-aluminum thermocouple; *6* – pressure vessel; *7* – valve; *8* – metallic glass to fill solutions; 9 – 2500 pressure vessel; *10* – uninvestigated sample; *11* – apolyethylene bag; *12* – the Dewar vessel; *13* – valve; *14* – capillary tube (stainless steel); *15* – ammeter; *16* – voltmeter; *17* – potentiostat (LATR); *18* – stabilizer; *19* – copper cylinder with nichrome heater; *20* – thermocouple junction

### 2.4. *Experimental setup for measuring the specific heat capacity of solutions under high state parameters*

To measure the heat capacity of liquids under high temperatures and pressures the experimental setup was used according to the method of monotonous heating [14–15, 21–22].

Professor M.M. Safarov's setup basically consists of a measuring cell (container) *1*, a chamber (the pressure container) of high pressure *6* and electrical measuring devices *15*, *16* (Fig. 3). The measuring cell *1* is placed into the copper glass *19* on which the nichrome heater is wound *3*. Through the thin-walled stainless steel tubes the measuring cell *1* is connected with the pressure vessel *6*. The heater *3* and the hot junction of the thermocouple *20* are under atmospheric pressure. When measuring we used the differential chrome-aluminium thermocouple with a diameter of 0.15 mm, the ends of which were connected to the graph plotter *2*. The cold junction of the differential thermocouple was placed into the Dewar vessel with melting ice and the hot junction touched the body of the measuring cell *1*. To measure the specific heat capacity under high pressure and high temperature the setup was equipped with a cylindrical electric furnace *3*. Its outer diameter is 34 mm and its inner diameter is 24 mm. On the outer surface of the electric furnace there is an electric heater in the form of a spiral made of the nichrome wire with a diameter of 1 mm. Asbestos was used as insulation. The electric furnace was insulated from the outside and from the ends. The electric furnace was powered by the laboratory transformer (LATR) *17* and the stabilizer *18*. Current and voltage were measured by an ammeter *15* and voltmeter *16*. In this setup the pressure vessel was used for measuring the thermal conductivity of the solutions under various temperatures and pressures. To verify the correctness of the experiment procedure the test measurings were carried out with toluene, *n*-hexane and kerosene. The specific heat capacity of the control samples under atmospheric pressure was measured in the temperature range 273–373 K. The experimental values of specific heat capacity of the control samples are shown in Fig. 4. This graph also shows the data from [13]. As you can see, the experimental data on the specific heat capacity of

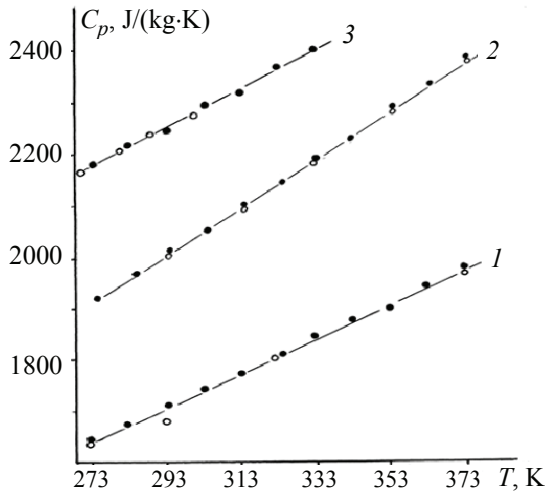


**Fig. 4. The comparison of experimental values of the samples heat capacity with the following data [1]:**
*1* – toluene; *2* – kerosene; *3* – *n*-hexane; ● – the author's data; o – data [1]

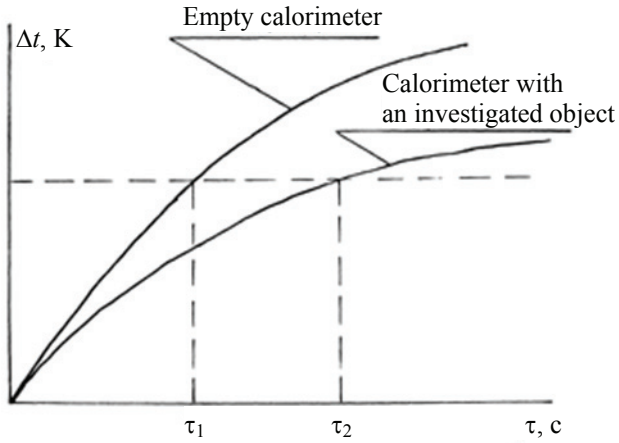


**Fig. 5. The dependence of temperature Δ*t* in the measuring unit on time τ**

toluene, *n*-hexane and kerosene coincide with the data from [13] through the whole temperature range. Being sure that the equipment qualitatively and quantitatively reproduces the heat capacity of the control samples depending on temperature and pressure we started to measure the specific heat of test objects.

**The procedure for measuring the specific heat**. When the valves *7* are closed, the test solution is poured into the glasses *8*. Then the valves *7* are opened and after filling the measuring cell (container) with test solution they are closed again .

The required pressure is formed by the MP-2500 deadweight tester through the pressure vessel in the device. Then the electric furnace circuit is switched on and simultaneously the H-306 graph plotter is switched on too. Each measuring of the heat capacity allowed obtaining a graph which is shown in Fig. 5. Thus, by comparing two graphs, the specific heat capacity of the test solutions is calculated.

### 2.5. *Formulas for calculating the specific heat capacity of solutions on the basis of experimental data*

The specific heat capacity of the test solutions according to the experimental data (Fig. 2 and 3) was calculated using the following formula:

$$C_p = \frac{\tau_x\left(m_1C_1 + B + K\tau_{\text{av}}\right) - \tau_1\left(B + K\tau_{\text{av}}\right)}{\tau_1 m_x}, \qquad (6)$$

where $m_x$ – test liquid mass; $m_1$ – calibration liquid mass; $\tau_{\text{av}} = \frac{\tau_1 + \tau_2}{2}$, $\tau_1$ – heating time of the calibration liquid, $\tau_2$ – heating time of test liquid; $B = 40{,}93$ and $K = -0{,}04$ – are the constants determined by measuring the thermal conductivity of the calibration liquid under the constant heating power.

Formula (6) eliminates the influence of the parasitic heat flows on measuring the specific heat due to the introduction of permanent measuring cells.

The heat capacity of test solutions according to the experimental data (Fig. 3) in a wide range of temperatures and pressures is calculated by the formula:

$$C_p = \frac{I^2 R\Delta\tau}{m\Delta T}, \qquad (7)$$

where $I$ – is current intensity; $R$ – resistance of the heater; $m$ – mass of test objects; $\Delta T$ – difference of temperatures; $\Delta\tau$ – the change in temperature of the measuring cell in time $\Delta\tau$.

### 2.6. *Calculation of measurement inaccuracy of the specific heat capacity of the investigated solutions*

According to Eq. (6) the confidence interval limit error of measuring the specific heat capacity is determined from the ratios [3, 4, 16, 19, 20, 24, 25]

$$\Delta C_p = \left(\left(\frac{\partial C_p}{\partial B}\right)^2(\Delta\tau_x)^2 + \left(\frac{\partial C_p}{\partial m_1}\right)^2(\Delta m_1)^2 + \right.$$
$$+\left(\frac{\partial C_p}{\partial C_1}\right)^2(\Delta C_1)^2 + \left(\frac{\partial C_p}{\partial B}\right)^2(\Delta B)^2 + \left(\frac{\partial C_p}{\partial K}\right)^2(\Delta \text{K})^2 +$$
$$\left.+\left(\frac{\partial C_p}{\partial \tau_{\text{cp}}}\right)^2(\Delta\tau_{\text{cp}})^2 + \left(\frac{\partial C_p}{\partial m_x}\right)^2(\Delta m_x)^2 + \left(\frac{\partial C_p}{\partial \tau_1}\right)^2(\Delta\tau_1)^2\right)^{\frac{1}{2}}, \qquad (8)$$

where

$$\frac{\partial C_p}{\partial \tau_x} = \frac{m_1C_1 + B + K\tau_{\text{av}}}{\tau_1 m_x}; \qquad (9)$$

$$\frac{\partial C_p}{\partial m_1} = \frac{\tau_x C_1}{\tau_1 m_1}; \qquad (10)$$

$$\frac{\partial C_p}{\partial C_1} = \frac{\tau_x m_1}{\tau_1 m_x}; \qquad (11)$$

$$\frac{\partial C_p}{\partial B} = \frac{\tau_x - \tau_1}{\tau_1 m_x}; \qquad (12)$$

$$\frac{\partial C_p}{\partial \text{K}} = \frac{\left(\tau_x - \tau_1\right)\tau_{\text{av}}}{\tau_1 m_x}; \qquad (13)$$

$$\frac{\partial C_p}{\partial m_x} = \frac{\tau_1\left(B + K\tau_{\text{av}}\right) - \tau_x\left(m_1C_1 + B + K\tau_{\text{av}}\right)}{\tau_1\left(m_x\right)^2}; \qquad (14)$$

$$\frac{\partial C_p}{\partial \tau_1} = -\frac{\tau_x \left( m_1 C_1 + B + K\tau_{\text{av}} \right)}{\tau_1^2 m_x}. \qquad (15)$$

Using Eq. (6) and taking into account the ratios (8) – (15), the confidence limit error in measuring the specific heat capacity in the relative form with $\alpha = 0{,}95$ was calculated.

Information on the quantitative assessment of the $C_p$ error is shown in Table 1.

The calculations showed that the confidence limit of the error in measuring the specific heat capacity in the relative form with $\alpha = 0.95$ is 0.45 %, the procedure error is 1.37 % and the instrumental error is 1.18 %. The total relative error of $C_p$ is 3.0 %. The detailed calculation of a separate measuring error of the heat capacity is given in Appendix 2.

The error calculation of the measuring specific heat capacity (Fig. 3) is done in accordance with [3, 11, 14–16, 19–21, 24, 25].

Table 1

**Initial data to quantify the confidence limit of measurement error of thermal conductivity**

| No. | Data name | Value |
|---|---|---|
| 1 | The diameter of the calorimeter core $d$, m | $1.72 \cdot 10^{-2}$ |
| 2 | The error in determining the core diameter (by a micrometer) $\Delta d$, m | $5 \cdot 10^{-5}$ |
| 3 | Inner diameter of the calorimeter $d_2$, m | $1.85 \cdot 10^{-2}$ |
| 4 | The error in determining the diameter of the calorimeter $\Delta d_2$, m (indicating Alesometer NO-50A) | $5 \cdot 10^{-5}$ |
| 5 | The length of the calorimeter core $l$, m | $17 \cdot 10^{-2}$ |
| 6 | The error in determining the core length $\Delta l$, m | $1 \cdot 10^{-3}$ |
| 7 | The specific heat capacity of the material of measuring cylinder $C'_{\text{c}}$, J/(kg·K) | 391 |
| 8 | The error in determining the specific heat capacity of the measuring cylinder $\Delta C'_{\text{c}}$, J/(kg·K) | 4.5 |
| 9 | The total heat capacity of the core (of measuring cylinder) $C_{\text{c}}$, J/K | 137.0 |
| 10 | The error in determining the total heat capacity (of measuring cylinder) $\Delta C_{\text{c}}$, J/K | 4.2 |
| 11 | The total heat capacity of the investigated layer $C_{\text{l}}$, J/K | 5.36 |
| 12 | The error in determining the heat capacity of the investigated layer $\Delta C_{\text{l}}$, J/K | 0.03 |
| 13 | The regular cooling time $\tau$, c | 35 |
| 14 | The error in determining the cooling time $\Delta\tau$, c | 0.2 |
| 15 | The core mass $G_{\text{c}}$, kg | 0.35 |
| 16 | The error in measuring the core mass $\Delta G_{\text{c}}$, kg | $1 \cdot 10^{-4}$ |
| 17 | The layer mass $G$, kg | 0.032 |
| 18 | The error in determining the layer mass $\Delta G$, kg | $1 \cdot 10^{-4}$ |
| 19 | The density of the material of measuring cylinder $\rho$, kg/m$^3$ | 8920 |
| 20 | The error in determining the density of the measuring cylinder material $\Delta\rho$, kg/m$^3$ | 25 |
| 21 | The regular cooling pace $m$, 1/s | $14.7 \cdot 10^{-3}$ |
| 22 | The error in determining the regular cooling pace $\Delta m$, 1/c | $0.06 \cdot 10^{-3}$ |
| 23 | The experimental pressure $P$, MPa (MP–2500 deadweight tester) | 49.05 |
| 24 | The error in measuring pressure $\Delta P$, MPa | 0.005 |
| 25 | The value of the thermal conductivity of toluene $\lambda$, W/(m·K) | 0.135 |
| 26 | The confidence limit of the error of measuring in the relative form with $\alpha = 0.95$ % | 1.8 |
| 27 | The procedure error, % | 1.8 |
| 28 | The instrumental error, % | 1.8 |
| 29 | The total relative error of measurements, % | 5.4 |

According to Eq. (7) the confidence error limit of the results of measuring specific heat capacity is determined from the ratio:

$$\Delta C_p = \left( \left( \frac{\partial C_p}{\partial I} \right)^2 (\Delta I)^2 + \left( \frac{\partial C_p}{\partial R} \right)^2 (\Delta R)^2 + \left( \frac{\partial C_p}{\partial \tau} \right)^2 (\Delta \tau)^2 + \left( \frac{\partial C_p}{\partial m} \right)^2 (\Delta m)^2 + \left( \frac{\partial C_p}{\partial t} \right)^2 (\Delta t)^2 \right)^{\frac{1}{2}} \quad (16)$$

where

$$\frac{\partial C_p}{\partial I} = \frac{2IR\Delta\tau}{m\Delta t}; \quad (17)$$

$$\frac{\partial C_p}{\partial R} = \frac{I^2\Delta\tau}{m\Delta t}; \quad (18)$$

$$\frac{\partial C_p}{\partial \tau} = \frac{I^2R}{m\Delta t}; \quad (19)$$

$$\frac{\partial C_p}{\partial m} = \frac{I^2R\Delta\tau}{m^2\Delta t}; \quad (20)$$

$$\frac{\partial C_p}{\partial t} = -\frac{I^2R\Delta\tau}{m(\Delta t)^2}. \quad (21)$$

Using equations (6) and (7) and taking into account the ratios (16) – (21) the confidence limits of error of heat capacity in the relative form with $\alpha = 0.95$ were calculated.

The total confidence limit of measurement error of specific heat capacity with $\alpha = 0.95$ does not exceed 3.2 %. Initial data for calculating the heat capacity (Fig. 3) are presented in Table 1.

### 2.7. *The description of the experimental setup for measuring the specific heat capacity of investigated solutions in regular thermal regime*

To measure the specific heat capacity of solutions under atmospheric pressure ($T = 293$ K), we assembled the experimental setup working according to the second method of the regular thermal regime [12, 15, 21, 24].

This experimental setup is shown in Fig. 6. It consists of a cardboard tube *1* with a diameter of 40 cm and with a height of 1.5 m, a calorimeter *2*, a synchronous motor *3*, an impeller *4* and M 195/1 mirror galvanometer *9*. The tube *1* is placed on the cylindrical supports *6* and raised 15 cm above the floor. A fan which is rotated by a synchronous motor with a frequency of 3000 r/min is installed on the floor along the tube axis The fan creates the forced air flow and provides the condition $\alpha = \text{const}$. The conditions of $t = \text{const}$ are ensured by thermostating the premises.

The cylindrical measuring calorimeter is made of red copper and has the following dimensions: inner and outer diameters are equal to 29.5 and 31.5 mm, respectively, its height is 103 mm. The suspension is mounted on the upper end of the measuring calorimeter and the junction of a differential measuring thermocouple is inserted axially through this end (8). The hot junction of the differential thermocouple is inserted through the dual channel strip and is located along the axis of the measuring calorimeter, in its central part. The cold junction of a differential thermocouple is in the air flow at a distance of 1.5–2 cm from the calorimeter. The bottom end of the measuring calorimeter is threaded. The sample *5* is filled through the bottom open end of the measuring calorimeter and the copper stopper is screwed. The measuring calorimeter is placed in a chamber which is immersed into the TS-24 liquid thermostat. The measuring calorimeter and the sample in the thermostat are uniformly warmed up to the temperature which is 10–15 °C above the room temperature. After that, the chamber with a measuring calorimeter is removed from the thermostat and the calorimeter is suspended along the axis of the tube *1*, wherein the forced air flow is created.

The ends of the differential thermocouple *8* are connected to a mirror galvanometer *9*, through which the cooling rate of the measuring calorimeter *m* is determined.

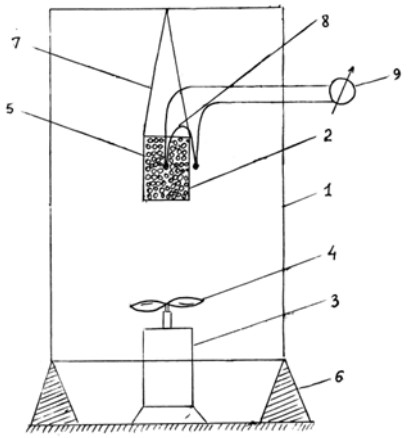


**Fig. 6. The experimental setup for measuring the specific heat capacity of solutions and powders under room temperature**

To determine the heat-transfer coefficient α we used a normal calorimeter which is a solid cylinder, made of red copper. Its height and diameter are the same as those of the measuring calorimeter. The hot junction of differential thermocouple is mounted into the normal calorimeter like in the measuring calorimeter *8*. The surface of the normal calorimeter is processed in the same way as the surface of the measuring calorimeter. The normal calorimeter is warmed up in a TS-24 thermostat and then is suspended along the axis of the tube *1* at the same distance from the fan like the measuring calorimeter.

The specific heat capacity $C_p$ of the samples is determined according to the formula [15, 22, 24]:

$$C_p = \frac{S\psi}{M_1}\left(\frac{\alpha}{m} - \frac{C_{\text{sh}}}{S}\right), \qquad (22)$$

where $S$ – is a surface of measuring calorimeter; $M_1$ – is a mass of the investigated sample; $C_{\text{sh}}$ – is a heat capacity of the shell of the measuring calorimeter; ψ – "criterion" value.

The field of temperatures of normal calorimeter is considered uniform and therefore the criterion ψ for it is equal to 1. In this case, the coefficient of heat dissipation α is determined by the formula:

$$\alpha = m_n \frac{C_n}{S}, \qquad (23)$$

where $m_n$ and $C_n$ – are the rate of cooling and the heat capacity of the normal calorimeter, respectively.

According to Eq. (22) we can calculate the specific heat capacity of the test sample on the basis of the experimental data.

### 3. Results and Discussion

As a pilot experiment the study of the dependence of the specific heat of the solution containing 90 % cottonseed oil and 10 % pure gasoline (wt. %) was carried out. The measurement results are shown in Table 2 which correspond to the results calculated by formula (7), indicating the correctness of the calculation according to (6) and measurement techniques in general.

Tables 3 and 4 show the results of determining thermal conductivity of the colloidal liquid hydrazine hydrate, both in pure form and containing fullerene ($C_{70}$), depending on temperature and pressure. Experiments were carried out on the measuring setup, the functional diagram of which is shown in Fig. 1.

Tables 3, 4 present the results of the experimental data on thermal conductivity of the investigated samples, depending on the temperature, pressure and concentration of fullerene ($C_{70}$; $d_{\text{av}}$ = 40 nm).

Tables 3 and 4 demonstrate that thermal conductivity of the fluid colloidal hydrazine hydrate both in pure form or containing fullerene $C_{70}$ decreases with increasing temperature, while the pressure increase leads to the drop of thermal conductivity of the liquid hydrazine hydrate.

For example, when the temperature is 293 K and the pressure changes in the range 0.101–49.01 MPa, the thermal conductivity of the colloidal system (hydrazine hydrate + 0.5 % $C_{70}$) increases by 47.4 %, when the temperature is 541.3 K it increases by 89.1 %, and when $T$ = 702.4 it increases 10-fold. It was found that the addition of 0.5 % $C_{70}$ in hydrazine hydrate when $T$ = 293 K and $P$ = 0.101 MPa increases its thermal conductivity by 28.9 %, under the temperature 702.4 K and the pressure $P$ = 49.01 MPa thermal conductivity increases by 32.6 %.

Table 2

**Comparison of the experimental and calculated (by a formula) values for specific heat capacity ($C_p$, J/(kg·K) of the solution (90 % cotton oil + 10 % pure gasoline (mass. %)) depending on temperature and pressure**

| $P$, MPa | 0.101 | | | 4.91 | | | 9.81 | | | 29.43 | | | 39.24 | | | 49.01 | | |
|---|---|---|---|---|---|---|---|---|---|---|---|---|---|---|---|---|---|---|
| | $C_p$ | | Δ, % | $C_p$ | | Δ, % | $C_p$ | | Δ, % | $C_p$ | | Δ, % | $C_p$ | | Δ, % | $C_p$ | | Δ, % |
| $T$, K | exp. | calc. | | exp. | calc. | | exp. | calc. | | exp. | calc. | | exp. | calc. | | exp. | calc. | |
| 291.4 | 1751 | 1674 | 4.4 | 1662 | 1646 | 1.0 | 1579 | 1556 | 1.5 | 1409 | 1384 | 1.8 | 1331 | 1302 | 2.2 | 1247 | 1209 | 3.1 |
| 310.6 | 1797 | 1780 | 0.9 | 1747 | 1732 | 0.9 | 1669 | 1649 | 1.2 | 1481 | 1410 | 1.4 | 1405 | 1384 | 1.5 | 1321 | 1300 | 1.6 |
| 331.7 | 1931 | 1900 | 1.6 | 1833 | 1803 | 1.6 | 1746 | 1716 | 1.7 | 1565 | 1534 | 2.0 | 1486 | 1472 | 0.9 | 1388 | 1357 | 2.2 |
| 348.2 | | | | 1895 | 1867 | 1.5 | 1806 | 1783 | 1.3 | 1628 | 1591 | 2.3 | 1546 | 1524 | 1.4 | 1458 | 1408 | 3.4 |
| 365.4 | | | | 1969 | 1962 | 0.4 | 1879 | 1852 | 1.4 | 1698 | 1684 | 0.8 | 1617 | 1600 | 1.1 | 1523 | 1501 | 1.4 |
| 390.4 | | | | 2084 | 2070 | 0.7 | 1993 | 1963 | 1.5 | 1805 | 1786 | 1.1 | 1718 | 1687 | 1.8 | 1620 | 1594 | 1.6 |
| 415.7 | | | | 2191 | 2171 | 1.0 | 2101 | 2082 | 0.9 | 1902 | 1889 | 0.7 | 1820 | 1784 | 2.0 | 1719 | 1702 | 1.0 |
| 440.1 | | | | 2299 | 2283 | 0.7 | 2208 | 2186 | 1.0 | 2018 | 2000 | 0.9 | 1939 | 1900 | 2.0 | 1837 | 1804 | 1.8 |
| 467.9 | | | | 2409 | 2384 | 1.0 | 2321 | 2300 | 0.9 | 2131 | 2102 | 1.4 | 2051 | 2005 | 2.2 | 1954 | 1903 | 2.6 |

Table 3

**Thermal conductivity ($\lambda \cdot 10^3$, W/(m·K)) of colloidal system (hydrazine hydrate + 0.1 % $C_{70}$) under different temperatures and pressures**

| $T$, K | Pressure $P$, MPa | | | | | | |
|---|---|---|---|---|---|---|---|
| | 0.101 | 4.91 | 9.81 | 19.62 | 29.43 | 39.24 | 49.1 |
| 293.3 | 462.3 | 490.8 | 508.7 | 580.4 | 601.7 | 640.5 | 680.3 |
| 313.4 | 430.4 | 480.3 | 490.1 | 570.6 | 590.3 | 630.7 | 674.4 |
| 331.5 | 420.2 | 458.6 | 575.2 | 550.3 | 578.1 | 620.0 | 660.2 |
| 353.6 | 400.8 | 426.7 | 454.7 | 535.7 | 566.8 | 600.8 | 640.3 |
| 373.0 | 380.3 | 408.3 | 432.5 | 523.7 | 550.5 | 585.7 | 630.0 |
| 395.4 | 360.5 | 390.5 | 416.3 | 512.4 | 530.6 | 575.3 | 610.4 |
| 423.2 | – | 360.2 | 390.2 | 486.7 | 510.3 | 550.4 | 590.3 |
| 448.5 | – | 330.4 | 370.6 | 460.2 | 500.4 | 536.7 | 570.0 |
| 468.0 | – | 312.6 | 350.3 | 450.3 | 480.6 | 526.8 | 558.4 |
| 486.7 | – | 290.3 | 322.6 | 430.9 | 470.2 | 510.8 | 540.0 |
| 503.3 | – | 270.5 | 312.4 | 422.0 | 450.3 | 480.7 | 525.0 |
| 523.0 | – | 255.4 | 300.2 | 415.2 | 440.5 | 470.3 | 518.6 |
| 541.4 | – | 230.0 | 280.3 | 395.4 | 430.0 | 462.0 | 500.1 |
| 558.0 | – | 220.3 | 270.0 | 380.2 | 412.6 | 450.3 | 480.2 |
| 573.2 | – | 206.2 | 255.3 | 370.1 | 402.0 | 440.1 | 470.2 |
| 598.1 | – | 180.4 | 230.4 | 358.3 | 370.5 | 415.6 | 460.0 |
| 618.4 | – | 175.5 | 220.6 | 350.0 | 365.2 | 408.5 | 440.3 |
| 638.0 | – | 168.3 | 212.4 | 348.3 | 363.5 | 400.0 | 430.1 |
| 658.3 | – | 167.5 | 201.6 | 346.4 | 360.7 | 395.4 | 427.2 |
| 673.0 | – | 164.6 | 200.0 | 344.7 | 358.9 | 390.7 | 420.2 |
| 693.2 | – | 155.8 | 198.2 | 340.5 | 356.4 | 388.7 | 418.5 |
| 723.2 | – | 150.0 | 196.7 | 336.9 | 351.7 | 388.0 | 416.7 |

Table 4

**Thermal conductivity ($\lambda \cdot 10^3$, W/(m·K)) of colloidal systems (hydrazine hydrate + 0.5 % $C_{70}$) under different temperatures and pressures**

| $T$, K | Pressure $P$, MPa | | | | | | |
|---|---|---|---|---|---|---|---|
| | 0.101 | 4.91 | 9.81 | 19.62 | 29.43 | 39.24 | 49.01 |
| 293.5 | 555.2 | 600.3 | 625.4 | 692.5 | 725.6 | 763.4 | 818.5 |
| 313.2 | 540.3 | 580.5 | 608.3 | 682.0 | 718.5 | 752.6 | 790.3 |
| 331.4 | 522.5 | 562.7 | 584.6 | 660.9 | 700.3 | 735.2 | 780.0 |
| 353.6 | 506.8 | 548.6 | 574.9 | 653.1 | 690.8 | 725.4 | 772.6 |
| 373.0 | 480.4 | 520.3 | 550.0 | 632.5 | 668.7 | 700.9 | 755.0 |
| 395.2 | 455.6 | 495.5 | 525.6 | 615.4 | 650.6 | 685.7 | 736.4 |
| 413.6 | – | 470.3 | 500.5 | 595.7 | 630.4 | 666.3 | 718.9 |
| 432.5 | – | 456.9 | 488.6 | 580.8 | 620.6 | 658.5 | 706.3 |
| 453.7 | – | 442.7 | 477.3 | 570.4 | 613.2 | 642.4 | 695.7 |
| 473.2 | – | 418.6 | 450.6 | 552.6 | 592.5 | 630.2 | 675.0 |
| 491.4 | – | 380.2 | 428.6 | 540.2 | 578.2 | 609.8 | 660.2 |
| 523.0 | – | 362.5 | 400.4 | 520.4 | 557.3 | 582.4 | 638.5 |
| 541.3 | – | 338.4 | 382.9 | 505.2 | 540.6 | 568.2 | 620.3 |
| 560.0 | – | 325.6 | 368.7 | 495.0 | 528.4 | 557.4 | 612.5 |
| 579.2 | – | 300.2 | 345.6 | 475.2 | 503.6 | 535.8 | 590.4 |
| 599.1 | – | 275.3 | 328.4 | 457.3 | 496.3 | 520.6 | 575.0 |
| 623.2 | – | 256.7 | 315.6 | 448.6 | 482.1 | 508.7 | 557.6 |
| 642.2 | – | 250.0 | 306.7 | 445.2 | 475.3 | 490.0 | 550.3 |
| 663.3 | – | 248.3 | 300.0 | 439.7 | 464.8 | 483.2 | 540.6 |
| 682.5 | – | 245.7 | 295.7 | 434.5 | 46079 | 480.9 | 536.9 |
| 702.4 | – | 243.8 | 292.6 | 431.6 | 458.7 | 477.6 | 530.4 |

To calculate specific heat capacity of liquid hydrazine hydrate containing nanostructured fullerene and carbon nanotubes with a diameter of 50 nm depending on the temperature and molar mass under atmospheric pressure the following approximated equation (24) was proposed:

$$C_p = \left[47.63 \cdot 10^{-2}\left(\frac{T}{T_1}\right)^2 - 81{,}93 \cdot 10^{-2}\left(\frac{T}{T_1}\right) + 1.353\right] \times \left[-32 \cdot 10^{-3}\left(\frac{m}{m_1}\right) + 1032 \cdot 10^{-3}\right] \times \left(-27.963 \cdot 10^3 \mu^2 + 6.999 \cdot 10^3 \mu + 3037.07\right), \text{ J/(kg·K)}. \quad (24)$$

Using equation (24) we can calculate the specific heat capacity of unexplored solutions (with the arithmetic average error of 0.3 % depending on the temperature under atmospheric pressure. For this purpose it is necessary to know only the mass value of concentration or molar mass.

Similarly, for calculating the temperature diffusivity, thermal conductivity and heat capacity of heat carriers depending on pressure the following equations were proposed:

$$a = \left[0.892\left(\frac{P}{P^*}\right)^2 - 1.123\left(\frac{P}{P^*}\right) + 1.232\right] \times \left(a\left(\frac{n}{n^*}\right)^2 + b\left(\frac{n}{n^*}\right) + c\right) \times \left(-1.52 \cdot 10^{-12}\left(\rho_1\right)^2 + 3.499 \cdot 10^{-9}\rho_1 - 1.88 \cdot 10^{-6}\right), \text{ s}^2/\text{m};$$

$$\lambda = \left[0.2844\left(\frac{P}{P^*}\right)^2 + 76.19 \cdot 10^{-3} \cdot 0.638\right] \times \left(a\left(\frac{n}{n^*}\right) + b\left(\frac{n}{n^*}\right) + c\right) \times \left(2.406 \cdot 10^{-5}\left(p_{\text{ж}}\right)^2 - 5.8 \cdot 10^{-2} p_1 + 35.253\right), \text{ W/(m·K)};$$

$$C_p = \left[0.299\frac{P}{P^*} - 1.165\frac{P}{P^*} + 1.866\right] \times \times \left(a\left(\frac{n}{n^*}\right) + b\frac{n}{n^*} + c\right) \times \times \left(0.206(\rho_l)^2 - 496.69\rho_l + 300568.04\right), \text{J/(kg·K)}, \quad (25)$$

where $\rho_l$ – is the density of heat carriers; *a*, *b* and *c* – are the coefficients of the equation (Tables 5–7).

Using Eq. (25) one can calculate the temperature diffusivity, thermal conductivity and heat capacity of the experimentally unexplored regions of heat carriers: antifreeze + carbon black, antifreeze + graphite, water + graphite, antifreeze + carbon nanotubes and water + carbon-nanotube depending on pressure under room temperature. For this purpose it is necessary to know only the values of density and concentration of heat carriers.

Table 5

**The coefficients (*a*, *b*, *c*) for the equation of temperature diffusivity (25)**

| Heat carrier | Coefficients | | |
|---|---|---|---|
| | *a* | *b* | c |
| Water + graphite powder | –0.94 | 0.7496 | 1.35 |
| Antifreeze + graphite powder | –1.306 | 1.652 | 0.865 |
| Antifreeze + carbon black | –0.4839 | 0.7103 | 0.8883 |
| Water + carbon nanotubes | –0.097 | –0.0563 | 1.108 |
| Antifreeze + carbon nanotubes | –0.32565 | 0.5301 | 0.8268 |

Table 6

**The coefficients (*a*, *b*, *c*) for the equation the thermal conductivity (25)**

| Heat carrier | Coefficients | | |
|---|---|---|---|
| | *a* | *b* | *c* |
| Water + graphite powder | –0.67 | 0.72752 | 0.85513 |
| Antifreeze + graphite powder | –1.9437768 | 2.3317729 | 0.7585789 |
| Antifreeze + carbon black | –0.4342 | 0.7016265 | 0.7445 |
| Water + carbon nanotubes | –0.1676 | 0.1144348 | 1.0658697 |
| Antifreeze + carbon nanotubes | –0.326212 | 0.53943 | 0.8204 |

Table 7

**The coefficients (*a*, *b*, *c*) for the equation the heat capacity (25)**

| Heat carrier | Coefficients | | |
|---|---|---|---|
| | *a* | *b* | c |
| Water + graphite powder | 0.181625 | –0.2979 | 0.8355 |
| Antifreeze + graphite powder | –0.04379 | 0.2698 | 1.144848 |
| Antifreeze + carbon black | 0.147696 | –0.292434 | 1.171 |
| Water + carbon nanotubes | 0.538525 | –0.4866 | 0.6053 |
| Antifreeze + carbon nanotubes | –0.30528 | 0.448 | 1.6533 |

Verification of equations (25) showed that they describe the temperature diffusivity, thermal conductivity and heat capacity of the heat carriers under investigation in the range of pressures from atmospheric up to 0.141 MPa under the room temperature with the mean square error of 7.61 %.

It is known that liquids and solids have two basic mechanisms of thermal conductivity: by free electrons (electronic thermal conductivity) and by atomic vibrations (phonons or lattice thermal conductivity). Phonon thermal conductivity dominates in dielectrics, which are basically liquids, including clean water. Electronic thermal conductivity dominates in metals. To explain the reasons for the thermal conductivity increase in nanofluids containing particles of highly heat-conducting materials, researchers analyze several basic mechanisms: Brownian motion of nanoparticles; the formation of high thermal conductivity of the liquid layer (with a molecular level thickness) at the liquid-particle interface; ballast transfer of thermal energy within a single nanoparticle and between nanoparticles which occurs when they are in contact; and the effects of nanoparticle clustering [5–8, 17, 23, 26–31].

## References


1. Vargaftik, N.B. (1972) Spravochnik po teplofizicheskim svojstvam gazov i zhidkostej [Reference book on thermophysical properties of gases and liquids]. M.: Nauka (Rus)

2. Ginzburg, A.S. (ed.) (1990) Teplofizicheskie harakteristiki pishhevyh produktov [Thermal characteristics of foodstuffs. Reference book] M.: Agropromizdat (Rus)

3. Gordov, A.N. (ed.) (1981) Staticheskie metody obrabotki rezul'tatov teplofizicheskogo jeksperimenta [Static methods of the thermophysical experiment results processing. Textbook] L.: LITMO (Rus)

4. Zemin, V.S. (1980) Jeksperimental'noe issledovanie plotnosti predel'nyh spirtov pri razlichnyh temperaturah i davlenijah [Experimental study of the limit alcohol density under different temperatures and pressures. Phd thesis.] M. (Rus)

5. Estman, J.A. (ed.) (2004)Thermal transport in nenofluids. Annu. Rev. Mater. Res. Vol. 34. (Eng)

6. Hamilton, R.L. (ed.) (1962) Thermal conductivity of heterogeneous two component systems. I and EC Fundamentals Vol.1 (Eng)

7. Keblinsi, P. (ed.) (2002) Mechanisms of heat flow in suspensions of nano-sized particles (nanofluids). Inter. J. of Heat and Mass Transfer (Eng)

8. Kumar, D.H. (ed.) (2004) Model for heat conductivity in nanofluids. Physical Review Letter. Vol. 93. (Eng)

9. Kartavchenko, A.V. (ed.) (1987) Razrabotka kataliticheskogo paketa razlozhenija nizkozamerzajushhego topliva (tipa gidrazingidrata) dlja glubokovodnogo apparata «Okean» [Catalytic package development of antifreezing fuel decomposition] (such as hydrazine hydrate) for the deep-sea vehicle "Ocean"] NPO GIPH (Rus)

10. Kraussold, N. (1934) Fershung Uebiete Ungh. W. (Germ)

11. Kozlov, A.D. (1980) Razrabotka i vnedrenie v narodnoe hozjajstvo sistemy normativno spravochnyh dannyh o termodinamicheskih svojstvah tehnicheski vazhnyh gazov, zhidkostej i smesej [Development and implementation of standard reference data on the thermodynamic properties of technically important gases, liquids and mixtures into the national economy system. Doctoral dissertation abstract] M. (Rus)

12. Kondrat'ev, G.M. (1954) Reguljarnyj teplovoj rezhim [Regular thermal regime] M.: GITTL. (Rus)

13. Kondrat'ev, G.M. (1957) Teplovoe izmerenie [Thermal measuring] M.: Mashgiz (Rus)

14. Mustafaev, R.A. (1971) Pribor dlja izmerenija teploemkosti zhidkostej pri vysokih davlenijah v rezhime monotonnogo razogreva [Device for measuring the heat capacity of liquids under high pressures in the heating monotonic mode. Proceedings of the universities of the USSR. Instrument making] (Rus)

15. Mustafaev, R.A., Kurepin, V.V. (1973) Dinamicheskij metod izmerenija teploemkosti zhidkostej pri vysokih temperaturah i davlenijah [Dynamic method of the heat capacity measuring of fluids under high temperatures and pressures] TVT. (Rus)

16. Men', A.A., Sergeev, O.A. (1971) Luchisto-konduktivnyj teploobmen v srede s selektivnymi opticheskimi svojstvami [Radiant-conductive heat transfer in a medium with selective optical properties] TVT. (Rus)

17. Patel, H.E**.** (ed.) **(**2003) Thermal conductivities of naked and monolayer protected metal nanopaticale based nanofluids: Manifestation of anomalous enhancement and chemical effects. App. Phys. Lett.Vol. 83 (Eng)

18. Prasher, R. (ed.) (2006) Thermal conductivity of nanoscale colloidal solutions (nano fluids). Phys. Rev. Lett. Vol. 89 (Eng)

19. Parfenov, V.G. (1983) Regressionnyj i korreljacionnyj analiz. Obrabotka rezul'tatov nabljudenij pri izmerenijah [Regression and correlation analysis. Processing of the observations results in the measurements. Textbook]. L.: LITMO (Rus)

20. Rabinovich, S.G. (1970) Metodika vychislenija pogreshnosti rezul'tatov izmerenija [Methods of calculating the error of measurement results. Metrology] (Rus)

21. Safarov, M.M. (1993) Teplofizicheskie svojstva prostyh jefirov i vodnyh rastvorov gidrazina v zavisimosti ot temperatury i davlenija [Thermophysical properties of ethers and aqueous solutions of hydrazine, depending on the temperature and pressure. Doctoral dissertation]. Dushanbe (Rus)

22. Safarov, M.M. (1986) Teplofizicheskie svojstva okisi aljuminija s metallicheskimi napolniteljami v razlichnyh gazovyh sredah [Thermophysical properties of alumina with the metal fillers in various gas atmospheres. Phd thesis]. Dushanbe (Rus)

23. Terehov, V.I. (ed.) **(**2010) Mehanizm teploperenosa v nanozhidkostjah: sovremennoe sostojanija problemy (Obzor) [The mechanism of heat transfer in nanofluids: current state of the problem (Review). Synthesis and properties of nanofluids. Heat physics and Aeromechanics] (Rus).

24. Klimenko, A.V., Zorin V.M. (ed.) **(**2001) Teoreticheskie osnovy teplotehniki. Teplotehnicheskij spravochnik: Spravochnik [Theoretical basics of the heat engineering. Thermal Engineering Reference book.] M.: Izdatel'stvo MJeI (Rus).

25. Gerashhenko, O.A. (ed.) (1984) Temperaturnye izmerenija: Spravochnik [Temperature measurements: Reference book] Kiev: Nauk. Dumka (Rus)

26. Zhang, X. (2007) Effective thermal conductivity and thermal diffusivity of nanofluids containing spherical and cylindrical nanoparticles. Experimental Thermal and Fluid Science. Vol. 31, №6. (Eng)

27. Choi, S.U.S. (2009) Nanofluids: from vision to reality through research. J. of Heat Transfer. Vol. 131. (Eng)

28. Choi, S.U.S., Zang Z.G., Yu W. (2001) Anomalous thermal conductivity enhancement in nanotube suspensions. App.Phys.Lett.Vol.79. (Eng)

29. Shenogin, S., Budapati A., Xui L., Ozisiki R., Keblinsi P. (2004) Effect of chemical functionalization on thermal transport of carbon nanotube composites. App.Phys.Lett.,Vol. 85. (Eng)

30. Wang, B.-X., Zhou L.-P., Peng X.-F. (2003) A fractal model for predating the effective thermal conductivity of liquid with suspension of nanoparticles. Inter. J. of Heat and Mass Transfer. Vol. 46. (Eng)

31. Yu, W., Choi, S.U.S. (2003) The role of interfacial layers in the enhanced thermal conductivity of nanofluid: a rerenovated maxwel model. J. of Nanoparticle Research, №5 . (Eng)